

**Biophysical Journal, Volume 110**

**Supplemental Information**

**Quantitative Determination of the Probability of Multiple-Motor Transport in Bead-Based Assays**

**Qiaochu Li, Stephen J. King, Ajay Gopinathan, and Jing Xu**

**SUPPORTING MATERIAL**

**Quantitative Determination of the Probability of Multiple-Motor Transport in Bead-Based Assays**

Qiaochu Li,<sup>1</sup> Stephen J. King,<sup>2</sup> Ajay Gopinathan,<sup>1</sup> and Jing Xu<sup>1,\*</sup>

<sup>1</sup>Department of Physics, School of Natural Sciences, University of California, Merced, CA 95343, USA

<sup>2</sup>Burnett School of Biomedical Sciences, University of Central Florida, FL 32827, USA

\*Correspondence: Jing Xu (jxu8@ucmerced.edu)

**RUNNING TITLE:** Probability of Multiple-Motor Transport

**TABLE OF CONTENTS**

**SUPPORTING TEXT.....2**  
**SUPPORTING FIGURES.....6**  
**SUPPORTING REFERENCES.....9**

## SUPPORTING TEXT

### 1. Motile fraction indicates the average number of active motors on a bead

We used motile fraction as a direct readout for the average number of active motors on a bead (1, 2) (Fig. S2). Motile fraction refers to the probability of beads exhibiting motility along microtubules. While motile-fraction measurements do not require optical trapping, trap-free readout can be difficult to interpret due to the potential presence of dead motors that lack enzymatic activity but can still bind microtubules. When an optical trap is used to confine individual beads to the vicinity of the microtubule (as we did in the current study), the bead must move against the optical trap to demonstrate directed motion along the microtubule. A dead motor may bind the microtubule, but it cannot exert force to drive bead movement against the optical trap, and thus it cannot contribute to a motile event. The resulting motile fraction measurements are therefore not sensitive to the potential effect of dead motors, providing a direct readout for the average number of active motors on the bead.

### 2. Travel threshold selection

When a bead is transported by a single motor, the probability of measuring a travel distance of  $x$   $\mu\text{m}$  is described by the single exponential decay  $P(x) = e^{-x/d}$ , where  $d$  is the mean travel distance of a single motor. For the kinesin motor,  $d = 1 \mu\text{m}$  (1, 3), and the likelihood that single-kinesin travel persists for less than  $x_0$  is  $1 - e^{-x_0/d}$ . We thus expect that 99.9% of beads transported by a single kinesin travel  $\leq 6.9 \mu\text{m}$ .

### 3. Estimations using a previous theory model in reference (2)

A previous study (2) modeled the probability that a bead is transported by two or more motors as

$$P_{previous}(\geq 2) = \alpha \cdot (1 - e^{-n} - ne^{-n}),$$

where  $\alpha$  is the probability that two randomly attached motors on the bead are within simultaneous reach of the microtubule and  $n$  is the mean number of active motors available for bead transport. Motile fraction provides a direct experimental readout for  $n$  (Supporting Text 1 and Fig. S2).

For kinesin, the previous model estimated that  $\alpha = 0.099$ , given the bead size employed in this study and in typical optical trapping studies (500 nm diameter) (Fig. S1 A). Thus,

$$P_{previous}(\geq 2) = 0.099 \cdot (1 - e^{-n} - ne^{-n}).$$

In our study, we recast the dependence on the mean motor number ( $n$ ) as that on motile fraction, which we measured experimentally, using the relationship *motile fraction* =  $1 - e^{-n}$  (Fig. S2 and (1, 2)). Thus,

$$P_{previous}(\geq 2) = 0.099 \cdot (mf + (1 - mf) \cdot \ln(1 - mf)),$$

where  $mf$  denotes the motile fraction. Note that this probability considers all beads, including those that did not interact with the microtubule. We normalized  $P_{previous}(\geq 2)$  by the associated motile fraction to determine the probability that a motile event is carried out by two or more motors (magenta line, Fig. 1 B and Fig. 4, left).

A similar evaluation for dynein (magenta line, Fig. 4, right) was carried out by substituting  $\alpha = 0.039$  into the above expression (Fig. S1 A).

#### 4. Derivation of Equation 1 in the main text

The probability that a bead is transported by two or more motors is determined by the weighted sum  $P(\geq 2) = \sum_{k=2}^{\infty} p(k | n) \cdot g(2 | k)$ , where  $n$  is the average number of motors on the bead,  $p(k | n)$  is the Poisson probability that there are exactly  $k$  motors on the bead, and  $g(2 | k)$  is the probability that at least two of the  $k$  motors on the bead are available for transport.

Substituting in  $p(k | n) = n^k e^{-n} / k!$  and  $g(2 | k) = 1 - (1 - \alpha)^{k-1}$ , we obtain

$$\begin{aligned} P(\geq 2) &= \sum_{k=2}^{\infty} \left( \frac{n^k e^{-n}}{k!} \right) \cdot (1 - (1 - \alpha)^{k-1}) \\ &= \sum_{k=2}^{\infty} \frac{n^k e^{-n}}{k!} - \sum_{k=2}^{\infty} \frac{n^k e^{-n} (1 - \alpha)^{k-1}}{k!} \\ &= 1 - e^{-n} - n e^{-n} - e^{-n} \sum_{k=2}^{\infty} \frac{n^k (1 - \alpha)^{k-1}}{k!}. \end{aligned}$$

To derive a closed-form expression for  $P(\geq 2)$ , we denote the infinite sum in the above expression as  $S = \sum_{k=2}^{\infty} \frac{n^k (1 - \alpha)^{k-1}}{k!}$ . Note that  $S = 0$  when  $n = 0$ .

The derivative of  $S$  with respect to  $n$  gives rise to

$$\begin{aligned} \frac{dS}{dn} &= \frac{d}{dn} \left( \sum_{k=2}^{\infty} \frac{n^k (1 - \alpha)^{k-1}}{k!} \right) \\ &= \sum_{k=2}^{\infty} \frac{(n(1 - \alpha))^{k-1}}{(k - 1)!} \end{aligned}$$

$$\begin{aligned}
&= \sum_{k=1}^{\infty} \frac{(n(1-\alpha))^k}{k!} \\
&= \sum_{k=0}^{\infty} \frac{(n(1-\alpha))^k}{k!} - 1 \\
&= e^{n(1-\alpha)} - 1.
\end{aligned}$$

Integrating  $\frac{dS}{dn}$  yields  $S = \frac{e^{n(1-\alpha)}}{1-\alpha} - n + C$ . Since  $S = 0$  when  $n = 0$ ,  $C = -\frac{1}{1-\alpha}$  and

$$S = \frac{e^{n(1-\alpha)}}{1-\alpha} - n - \frac{1}{1-\alpha}.$$

Substituting the closed form for the infinite sum, we obtain Equation 1 in the main text,

$$P(\geq 2) = 1 + e^{-n} \left( \frac{\alpha}{1-\alpha} \right) - \frac{e^{-n\alpha}}{1-\alpha}.$$

## 5. Derivation of Equation 2 in the main text

Our experimental measurements represent lower-bound probabilities of multiple-motor transport, since our distance threshold excludes the population of multiple-motor transport events that travel  $\leq 6.9 \mu\text{m}$  (Fig. 1 in the main text). Imposing the same threshold, the expected lower-bound probability of multiple-motor transport is

$$P_{\text{lower-bound}}(\geq 2) = P(\geq 2) - \sum_{i=2}^{\infty} f_i \cdot P(=i),$$

where  $P(\geq 2)$  is the probability of multiple-motor events without imposing any travel threshold (Eq. 1 in the main text),  $P(=i)$  is the probability that the bead is transported by exactly  $i$  motors, and  $f_i$  is the probability that bead travel by exactly  $i$  motors is shorter than the travel threshold. We previously measured the value of  $f_2$  to be  $0.556 \pm 0.096$  for the experimental condition used in the present investigation (0.01 mM ATP) (4). Under the same experimental condition, the value of  $f_{i>2}$  approaches 0 based on predictions of multiple-motor travel distances by a theory model in (5). We thus have the following simplification,

$$P_{\text{lower-bound}}(\geq 2) = P(\geq 2) - f \cdot P(=2),$$

where  $f = f_2 = 0.556$  for simplicity.

The probability that a bead is transported by exactly two motors,  $P(=2)$ , is determined by

$$P(=2) = \sum_{k=2}^{\infty} p(k|n) \cdot \alpha \cdot (1-\alpha)^{k-2},$$

where  $n$  is the average number of motors on the bead,  $p(k | n)$  is the Poisson probability that there are exactly  $k$  motors on the bead,  $\alpha$  is the probability that two randomly attached motors are within simultaneous reach of the microtubule, and  $\alpha \cdot (1 - \alpha)^{k-2}$  is the probability that exactly two of the  $k$  motors on the bead are available for transport.

We derived a closed-form expression for  $P(= 2)$  as

$$\begin{aligned} P(= 2) &= \sum_{k=2}^{\infty} \frac{n^k e^{-n}}{k!} \cdot \alpha \cdot (1 - \alpha)^{k-2} \\ &= \frac{\alpha \cdot e^{-n}}{1 - \alpha} \sum_{k=2}^{\infty} \frac{n^k (1 - \alpha)^{k-1}}{k!} . \end{aligned}$$

Substituting  $\sum_{k=2}^{\infty} \frac{n^k (1 - \alpha)^{k-1}}{k!} = S = \frac{e^{n(1-\alpha)}}{1 - \alpha} - n - \frac{1}{1 - \alpha}$  from Supporting Text 4,

$$\begin{aligned} P(= 2) &= \frac{\alpha \cdot e^{-n}}{1 - \alpha} \cdot \left( \frac{e^{n-n\alpha}}{1 - \alpha} - n - \frac{1}{1 - \alpha} \right) \\ &= \frac{\alpha \cdot e^{-n\alpha}}{(1 - \alpha)^2} - \frac{\alpha \cdot n \cdot e^{-n}}{1 - \alpha} - \frac{\alpha \cdot e^{-n}}{(1 - \alpha)^2} . \end{aligned}$$

Thus,  $P_{lower-bound}(\geq 2) = P(\geq 2) - f \cdot \left( \frac{\alpha \cdot e^{-n\alpha}}{(1 - \alpha)^2} - \frac{\alpha \cdot n \cdot e^{-n}}{1 - \alpha} - \frac{\alpha \cdot e^{-n}}{(1 - \alpha)^2} \right)$ .

## SUPPORTING FIGURES

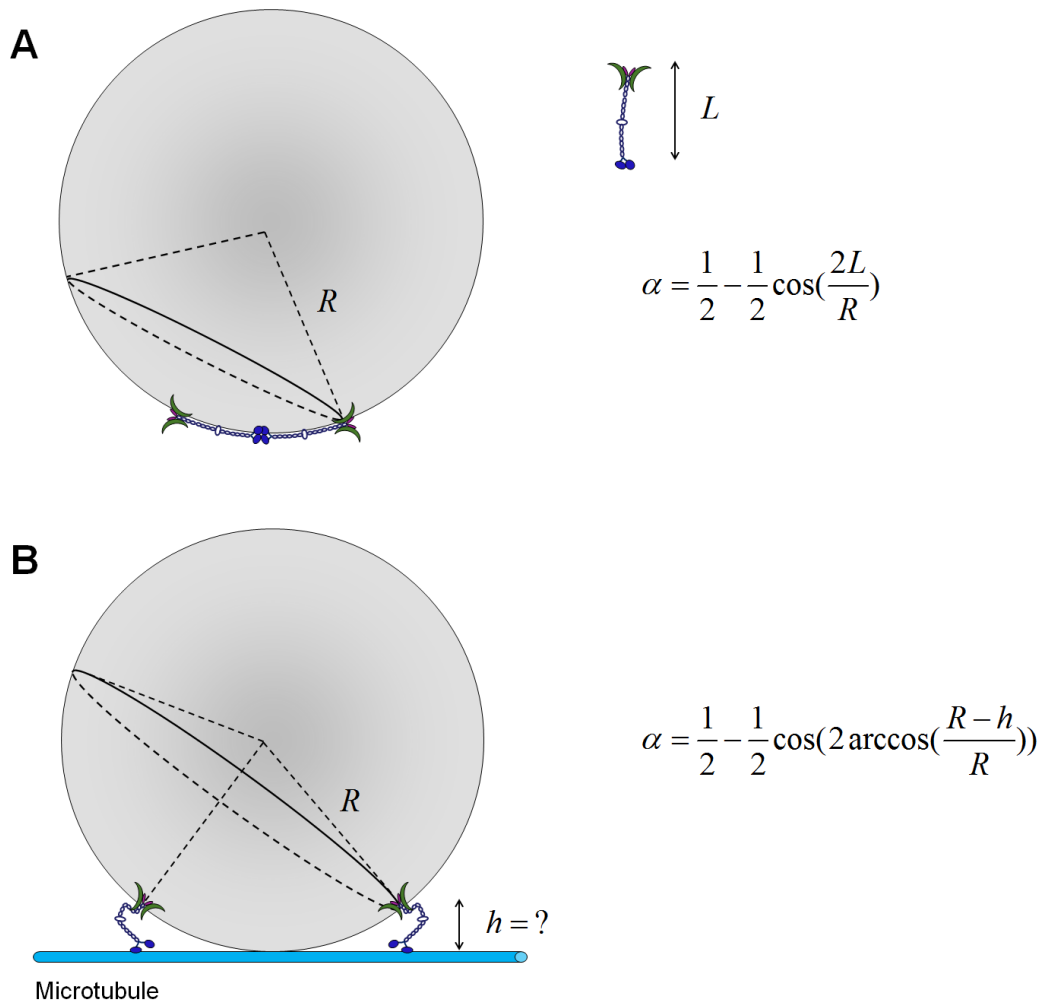


FIGURE S1 Geometries for two-motor transport (not to scale) and associated probability that two randomly attached motors are within simultaneous reach of the microtubule ( $\alpha$ ). Here we considered the condition in which the bead radius ( $R$ ) is larger than the motor's contour length ( $L$ ), and the motors are randomly distributed on the bead surface. Under this condition, although all motors on the bead can contribute to bead transport, not all motors can reach the microtubule at the same time. When any one motor on the bead binds the microtubule, there is a limited area surrounding this motor (a spherical cap) in which a second motor may be located and be within reach of the same microtubule. The value of  $\alpha$  is determined as the area ratio of this spherical cap to the entire bead surface. (A) Geometry for two-motor transport in a previous model (2). The motors are assumed to be fully extended, and their motor domains effectively in contact with each other. The area of the spherical cap enclosing a second motor available for transport has a radius twice the motor's contour length.  $R = 250$  nm in the current study (and in typical optical trapping studies). This geometry yields  $\alpha = 0.099$  for kinesin ( $L = 80$  nm (6, 7)) and  $\alpha = 0.039$

for dynein ( $L = 50$  nm (8, 9)). (B) An updated geometry for two-motor transport (10, 11). Here, the motors can bind different locations along the length of the microtubule, and the motors are no longer assumed to be fully extended. The area of the spherical cap enclosing a second motor available for transport is determined by  $h$ , the extension of the motor during active transport. There is limited information about  $h$  for flexible motors such as kinesin.



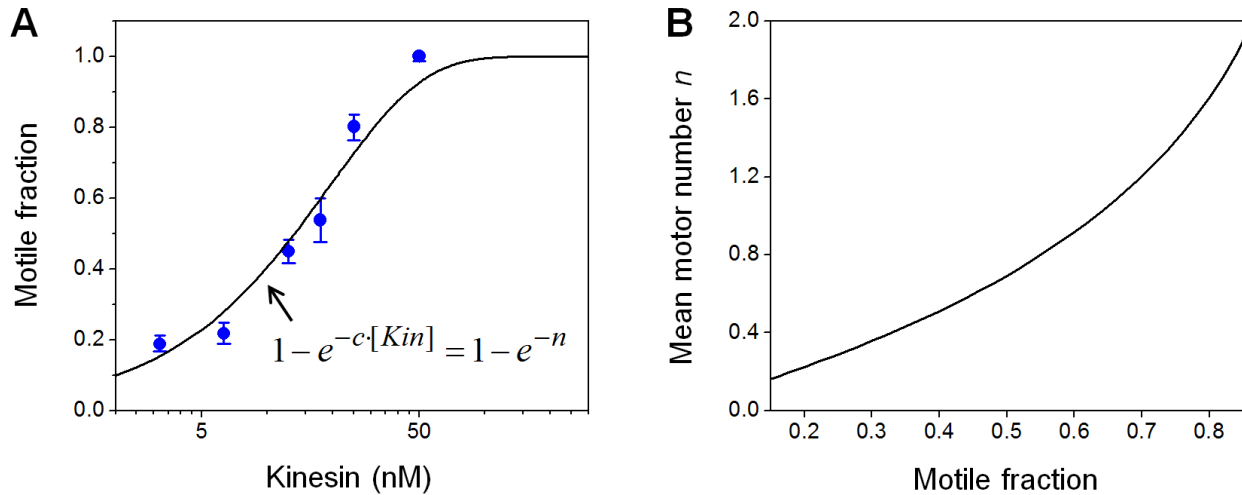


FIGURE S2 Motile fraction provides a direct experimental readout for the average number of active motors on the bead ( $n$ ). (A) Fraction of beads exhibiting motility along microtubules (“motile fraction”) as a function of kinesin motor concentration, measured using an optical trap and at 1 mM ATP. The concentration of beads was kept constant and the concentration of kinesin was varied. Individual beads were confined to the vicinity of microtubules with an optical trap (80-330 beads trapped for each motor concentration). Error bars represent standard error of the mean. Since motile fraction represents the probability that a bead is carried by at least one active motor, it is well described by the single-motor Poisson curve (1, 2)  $P(\geq 1) = 1 - e^{-c[Kin]} = 1 - e^{-n}$  (solid line), where  $c$  represents a fitting parameter and  $[Kin]$  indicates kinesin concentration. Note that, we carried out our measurements as a function of motile fraction rather than motor concentration ( $[Kin]$ ), because each motile fraction corresponds to a unique  $n$  value. In contrast, for any particular motor concentration ( $[Kin]$ ), the average number of active motors on a bead ( $n$ ) is not unique and depends sensitively on the concentration of beads used during motor/bead incubation (this dependence is reflected in the fitting parameter  $c$ ). (B) Relationship between  $n$  and motile fraction using  $motile\ fraction = 1 - e^{-n}$  (panel A and (1, 2)).

**SUPPORTING REFERENCES**

1. Block, S. M., L. S. Goldstein, B. J. Schnapp. 1990. Bead movement by single kinesin molecules studied with optical tweezers. *Nature* 348:348-352.
2. Svoboda, K., S. M. Block. 1994. Force and velocity measured for single kinesin molecules. *Cell* 77:773-784.
3. Yajima, J., M. C. Alonso, R. A. Cross, Y. Y. Toyoshima. 2002. Direct long-term observation of kinesin processivity at low load. *Curr Biol* 12:301-306.
4. Xu, J., Z. Shu, S. J. King, S. P. Gross. 2012. Tuning multiple motor travel via single motor velocity. *Traffic* 13:1198-1205.
5. Klumpp, S., R. Lipowsky. 2005. Cooperative cargo transport by several molecular motors. *Proc Natl Acad Sci U S A* 102:17284-17289.
6. Hirokawa, N., K. K. Pfister, H. Yorifuji, M. C. Wagner, S. T. Brady, G. S. Bloom. 1989. Submolecular domains of bovine brain kinesin identified by electron microscopy and monoclonal antibody decoration. *Cell* 56:867-878.
7. Scholey, J. M., J. Heuser, J. T. Yang, L. S. Goldstein. 1989. Identification of globular mechanochemical heads of kinesin. *Nature* 338:355-357.
8. Vallee, R. B., J. S. Wall, B. M. Paschal, H. S. Shpetner. 1988. Microtubule-associated protein 1C from brain is a two-headed cytosolic dynein. *Nature* 332:561-563.
9. Sakakibara, H., H. Kojima, Y. Sakai, E. Katayama, K. Oiwa. 1999. Inner-arm dynein c of *Chlamydomonas flagella* is a single-headed processive motor. *Nature* 400:586-590.
10. Walcott, S., P. M. Fagnant, K. M. Trybus, D. M. Warshaw. 2009. Smooth muscle heavy meromyosin phosphorylated on one of its two heads supports force and motion. *J Biol Chem* 284:18244-18251.
11. Korn, C. B., S. Klumpp, R. Lipowsky, U. S. Schwarz. 2009. Stochastic simulations of cargo transport by processive molecular motors. *J Chem Phys* 131:245107.